IEEE Access
Multidisciplinary ⋮ Rapid Review ⋮ Open Access Journal

Received December 22, 2020, accepted January 1, 2021, date of publication January 13, 2021, date of current version January 22, 2021.

Digital Object Identifier 10.1109/ACCESS.2021.3051385

Analysis of D2D-Aided Underlaying Uplink Cellular Networks Using Poisson Hole Process

WENYAN SHI[1], ZHI ZHANG[1], (Member, IEEE), YUZHEN HUANG[1,2], (Member, IEEE), AND WENJUN XU[3], (Senior Member, IEEE)

[1]State Key Laboratory of Networking and Switching Technology, Beijing University of Posts and Telecommunications, Beijing 100876, China
[2]Artificial Intelligence Research Center, National Innovation Institute of Defense Technology, Beijing 100166, China
[3]Key Laboratory of Universal Wireless Communications, Ministry of Education, Beijing University of Posts and Telecommunications, Beijing 100876, China

Corresponding author: Zhi Zhang (zhangzhi@bupt.edu.cn)

This work was supported in part by the National Natural Science Foundation of China under Grant 61971474, in part by the Beijing Nova Program under Grant Z201100006820121, and in part by the China Postdoctoral Science Foundation Funded Project under Grant 2019T120071.

ABSTRACT As one of the key technologies in 5th generation mobile networks, device-to-device (D2D) communication technology can significantly improve spectrum utilization, throughput and energy efficiency as well as reduce congestion in the networks. However, due to the spectrum sharing between D2D users (DUs) and cellular users (CUs), it may also cause serious interferences. In this paper, we adopt appropriate stochastic geometric tools to model and analyze the mutual interferences, based on which the coverage probabilities of different users are derived to evaluate the network performance. Specifically, we model the locations of CUs as a Poisson point process (PPP), while the locations of DUs are modelled as a Poisson hole process (PHP), which is driven by the PPP of CUs' locations due to the exclusion between the positions of CUs and DUs. Furthermore, the approximated expressions of user coverage probabilities are obtained by two methods, which are consistent with the simulation results. The first method is to dissolve the hole, and the second method is to approximate the PHP through a thinned PPP. In addition, the user ergodic data rates and the sum data rate of the networks are also derived through the second approach. The impacts of key parameters (such as the density of DUs and the size of the warning radius) on the ergodic rates and sum data rate are analyzed.

INDEX TERMS Coverage probability, sum data rate, Poisson hole process, D2D, stochastic geometry.

I. INTRODUCTION

In the past few years, with the explosive growth in the number of smart devices, the existing wireless communication networks are difficult to meet the users' demand for data rates. The technique of device-to-device (D2D) communication, which allows two proximate users to communicate directly by sharing the same spectrum with cellular users (CUs) without the relay of base station (BS), can improve spectrum utilization, network throughput and energy efficiency as well as alleviate the congestion for cellular networks by offloading some traffic [1]. Therefore, D2D communication has attracted widespread attention in the academia and industry. The authors of [2] investigated the impact of mode selection on the effective capacity of D2D communication. Besides, the work in [3] proposed a novel framework for mobile crowdsensing applications that combined D2D technologies with a C-RAN communication system, which helped to solve the delay issue and achieve most of the goals of 5th generation mobile networks in terms of delay, capacity, energy efficiency, mobility, and cost.

Despite the above benefits, the introduction of D2D communication into cellular networks will bring complex interference problems. Hence, how to use mathematical tools to model the mutual interferences reasonably and analyze the system performance based on the achieved interference model has become a research hotspot. Since the authors in [4] successfully analyzed the coverage probability of cellular networks, many researchers began to utilize stochastic geometry [5] with the Poisson point process (PPP) to model and analyze the system performance of wireless network [6]–[11]. Different from the traditional grid-based model, the PPP can describe the random characteristics of the nodes distribution in the networks accurately. Based on the tractability of PPP,

The associate editor coordinating the review of this manuscript and approving it for publication was Ahmed Mohamed Ahmed Almradi.

various expressions of network performance can be easily derived through transformations. The work in [6] used PPP to model the positions of macro-cell BSs in the heterogeneous cellular networks, and derived the analytical expressions about the success probability and energy efficiency. In [7], the authors derived the closed-form expression of the CUs' coverage probability and the corresponding number of potential D2D users (DUs) using stochastic geometry. Also, by means of stochastic geometry, in [9], the performance of D2D communication with full-duplex mode was investigated in detail. Meanwhile, in [10], the authors studied the performance of ultra-dense networks backed by a stochastic geometry model. In addition, the closed-form expressions of coverage probability and sum data rate were derived based on PPP in [11], and the maximum throughput was obtained through balancing the scale factor between DUs and all users in the underlaying cellular networks.

However, the PPPs model assume the locations of diffrent nodes are independent, while in reality, the positions of BSs and different users may be correlated to each other. For example, in order to ensure the quality of service (QoS), different nodes cannot be too close nor too far with each other. In other words, the assumption that the nodes are independent of each other in PPPs model does not reflect the real nodes distribution. In view of this observation, researchers have designed more accurate methods to describe the distribution of nodes, including the Poisson hole process (PHP), which is generated from two independent homogeneous PPPs. In a PHP, one PPP is utilized to represent the baseline PPP from which the holes are carved out and the other represents the locations of the holes. Obviously, this results in the analysis of PHP modelling being very difficult compared to PPP. To solve it, there are mainly three traditional methods by approximating the PHP to the PPP [12]. Recently, in [13], different from the traditional methods, the authors investigated the accurate upper and lower bounds of the Laplacian of the interference, which made great contributions to the performance analysis of PHP-based wireless networks. In [14], the lower bounds of the communication distances distribution in PHP were obtained, which made the research on PHP-based wireless networks more insightful.

Since PHP is more suitable for modelling and analyzing the wireless cellular networks, it has received a lot of attention from academia. For instance, PHP can be well used to model the locations of macro base stations and micro base stations in a two-tier heterogeneous network [15]–[17]. In consideration of protecting the privacy of primary users, it can also be employed to model the locations of the primary and secondary users in cognitive radio networks [18], [19]. In addition, PHP is involved in modelling the locations of DUs in D2D-aided cellular networks, and the corresponding network performance analyses were shown in [20], [21]. The work in [20] took the spectrum sensing ability of DUs into account and modelled the locations of DUs as the superposition of a PPP and a PHP. In [21], the authors assumed the DUs to form clusters, and then used Poisson cluster process (PCP) to model the positions of DUs as well as modelled the cluster centers as PHP in the downlink cellular networks.

Although the D2D-aided networks are considered in previous works [7], [11], [22]–[24], they both used two independent PPPs to model the locations of CUs and DUs, respectively. This did not reflect the true node distributions due to the exclusion between the positions of CUs and DUs. Furthermore, the works [20], [22] considered the special network scenarios, where D2D devices have special abilities, such as spectrum sensing and energy harvesting. The work [21] used PCP to model the positions of DUs. However, due to the close distance among DUs, their mutual interferences in the networks were serious. The works [23], [24] focused on modelling the disaster area networks, where the D2D devices play the role of relay and provide a disaster relief solution.

Motivated by the above discussion, in this paper, we consider a more general D2D-aided underlying uplink cellular networks, where the exclusion between the positions of CUs and DUs is considered and a new analysis framework based on the PPP-and-PHP hybrid model is adopted. Specifically, in order to protect both the QoS of CUs and DUs, the locations of CUs are modelled as a PPP, while the locations of DUs are modelled as a PHP, which is driven by the PPP of CUs' locations. In addition, according to the model way, we provide a detail mathematical analysis of coverage probability, ergodic data rate and the sum data rate, which provide an efficient way to evaluate the impacts of the density of DUs, and the size of the warning radius on the system performance. The main contributions of this paper are summarized as follows:

- We design a new analysis framework for the D2D-aided underlaying uplink cellular networks based on the PPP-and-PHP hybrid model, which is suitable for modelling and analyzing the spectrum sharing networks, such as D2D cellular networks. Driven by the CUs' locations being modelled by a PPP, the locations of DUs are modelled as a PHP due to the repulsive nature between CUs and DUs. That is, the DUs are not permitted to transmit when they fall into the neighborhood of CUs. Moreover, the cases of non-orthogonal and orthogonal frequency division multiplexing for CUs are both taken into account for a more comprehensive analysis of the network performance in the hybrid model.
- For the designed framework, two methods are adopted to analyze the system performance. The core idea of the first method is to dissolve the hole, while in the second method, we approximate the PHP with a PPP of the same density. Furthermore, the approximated expressions of the coverage probabilities of CUs and DUs are derived by the two methods, which are consistent with the simulation results and make us evaluate the impacts of the key parameters (e.g., the DUs' density and the size of the warning radius) on the performance of the networks more intuitively.
- Depending on the second method, we also derive the approximated expressions for the ergodic data rates of CUs and DUs as well as the sum data rate of the

entire networks. The obtained expression of the network throughput is conducive to comprehensive network performance evaluation and further optimization analysis. In addition, simulations are carried out to validate the accuracy of the analytical expressions based on the PPP-and-PHP hybrid model, and the comparison with the previous work based on PPPs model is also provided.

The rest of this paper is organized as follows. The designed PHP-based model for the D2D-aided underlaying cellular networks is introduced in Section II. In Section III, we give comprehensive analyses of the coverage probabilities for CUs and DUs based on two methods. After that, the ergodic data rates of different users and the sum data rate of the entire networks are obtained in Section IV. Section V demonstrates the simulation results and discusses them in detail. Finally, the paper is concluded in Section VI.

Notations: The probability of an event is denoted by $\mathbb{P}\{\bullet\}$, and the expectation of random variable x is expressed as $\mathbb{E}[x]$. The $\mathcal{L}(\bullet)$ represents the Laplace transforms of a random variable.

II. SYSTEM MODEL

As illustrated in Fig. 1, we consider a radius-R coverage D2D-aided cellular networks with one BS in the center, where M cellular users and K D2D pairs share the same one of the licensed uplink spectra.[1] Accordingly, $M > 1$ means using non-orthogonal frequency division multiplexing among CUs, while $M = 1$ stands for the orthogonal frequency division multiplexing manner which leads to other CUs in the networks having to utilize other spectrum units. As it is known, there is a certain exclusion between the positions of CUs and DUs. When DUs choose to reuse the spectrum resource, to guarantee their own QoS or CUs' QoS, they prefer to stay away from CUs. Therefore, the warning areas (holes) with radius D are assumed near all CUs, and the DUs which fall into these holes are not permitted to reuse the same spectrum. As a result, there will be $(K - N)$ D2D pairs failed to establish connections and the remaining N D2D pairs outside these holes in the networks will keep active. Next, we will discuss the system model in detail from the aspects of network architecture, communication link modelling and interference analysis.

A. NETWORK ARCHITECTURE

Under the above conditions, the M CUs are spatially distributed according to the model of classical homogeneous PPP Φ_c of density λ_c. Similarly, the locations of all K DUs are also modelled as a homogeneous PPP Φ_d of density λ_d'. Thus, the locations of the active N DUs outside the holes are modelled as a PHP $\Phi_h\left(\lambda_c, \lambda_d', D\right)$ of density λ_d, which consists of the above two independent homogeneous PPPs, i.e., Φ_d and Φ_c, to denote the baseline PPP and the locations of the holes, respectively. Actually, after the distribution of users has been modelled by the PPP-and-PHP hybrid model in each round, it is similar to the distance-constrained D2D-aided communications. However, we intend to obtain the expressions of some key metrics of particular interest to network designers, such as coverage probabilities and ergodic data rates of users, as well as the sum data rate of the networks. Specifically, we assume that each D2D transmitter (DT) has a D2D receiver (DR) at a fixed distance d_{tr} in a random direction. Accordingly, the number of CUs and active DUs in a single cell can be modelled as Poisson distributed random variables with expectations of $\mathbb{E}[M] = \lambda_c \pi R^2$ and $\mathbb{E}[N] = \lambda_d \pi R^2$, respectively.

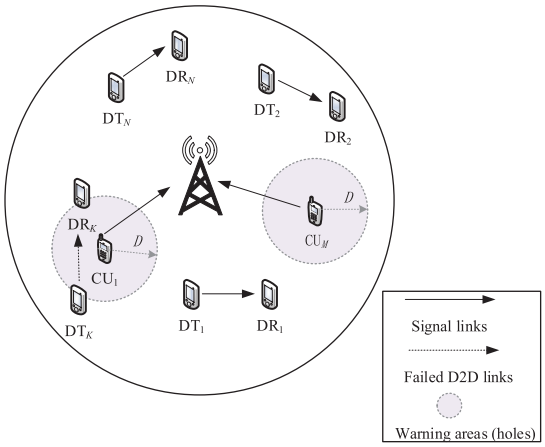

FIGURE 1. PHP-based uplink system model for the D2D-aided underlaying cellular networks.

Without loss of generality, for the channel between any two users, the standard power-law propagation model is used with pathloss exponent α, and small-scale channel fluctuations are modelled using Rayleigh fading. The CUs and the DTs are assumed to keep constant transmit powers of P_c and P_d, respectively. For the sake of simplifying notations, the subscripts o and k $(k = 1, 2, \ldots, M)$ are used in the following to represent the BS and the k-th CU, respectively. Meanwhile, the subscripts i $(i = 1, 2, \ldots, N)$ and j $(j = 1, 2, \ldots, N)$ are adopted to denote the i-th DT (i.e., the DT of the i-th D2D pair) and the j-th DR (i.e., the DR of the j-th D2D pair), respectively. For example, $d_{k,o}$ and $h_{k,o}$ represent the distance and the channel attenuation coefficient from k-th CU to the BS, respectively. Similarly, $d_{i,j}$ and $h_{i,j}$ denote the distance and the channel attenuation coefficient from the i-th DT to the j-th DR, respectively. Especially, $h_{j,j}$ denotes the channel attenuation coefficient of the j-th D2D pair.

B. SINR ANALYSIS

Since there are M CUs and N DUs sharing the same licensed uplink spectrum in a given cell, we just consider the interferences imposing on BS and DRs, including both inter-CU and inter-DU interferences. Specifically, at the BS, the received

[1] In our scenario, we think about the omnidirectional cellular networks, and the concept of a cell can be physically abstracted as a zone. When a cell is divided into several sectors, the interferences of CUs between different sectors can be avoided. However, each sector may still have multiple CUs multiplexing the same spectrum. Therefore, each sector can also be physically equivalent to a zone, and our methods can be applied to the analysis and derivation of each sector.

signal can be expressed as

$$y_o = \sum_{k=1}^{M} \sqrt{d_{k,o}^{-\alpha} P_c} \cdot h_{k,o} \cdot x_k + \sum_{i=1}^{N} \sqrt{d_{i,o}^{-\alpha} P_d} \cdot h_{i,o} \cdot x_i + N_0, \quad (1)$$

where x_k and x_i denote the signals transmitted by the k-th CU and the i-th DT, respectively. The N_0 denotes the additive white Gaussian noise (AWGN) at the receiver with $\mathcal{CN}\left(0,\ \sigma^2\right)$. Thus, the corresponding SINR of the BS from the k-th CU can be given by

$$\mathrm{SINR}_k = \frac{P_c d_{k,o}^{-\alpha} \left|h_{k,o}\right|^2}{I_d + I_c + \sigma^2}, \quad (2)$$

where $I_d = \sum_{i \in \Phi_h} P_d d_{i,o}^{-\alpha} \left|h_{i,o}\right|^2$ is the cumulative interferences caused by all active DTs in the Φ_h. $I_c = \sum_{k' \in \Phi_c / \{k\}} P_c d_{k',o}^{-\alpha} \left|h_{k',o}\right|^2$ is the cumulative interferences caused by other CUs, and k' denotes the CUs in the Φ_c except the k-th CU.

Similarly, the signal received at the j-th DR is

$$y_j = \sum_{k=1}^{M} \sqrt{d_{k,j}^{-\alpha} P_c} \cdot h_{k,j} \cdot x_k + \sum_{i=1}^{N} \sqrt{d_{i,j}^{-\alpha} P_d} \cdot h_{i,j} \cdot x_i + N_1, \quad (3)$$

where N_1 denotes AWGN at the j-th DR with $\mathcal{CN}\left(0,\ \sigma^2\right)$. Hence, the corresponding SINR can be given by

$$\mathrm{SINR}_j = \frac{P_d d_{tr}^{-\alpha} \left|h_{j,j}\right|^2}{I_d' + I_c' + \sigma^2}, \quad (4)$$

where $I_d' = \sum_{i \in \Phi_h \setminus \{j\}} P_d d_{i,j}^{-\alpha} \left|h_{i,j}\right|^2$ is the cumulative interferences from all active DTs in the Φ_h except the j-th DT, and $I_c' = \sum_{k \in \Phi_c} P_c d_{k,j}^{-\alpha} \left|h_{k,j}\right|^2$ is the cumulative interferences from all CUs in the Φ_c

III. COVERAGE PROBABILITY ANALYSIS

In this section, we will introduce two approaches to derive the user coverage probabilities with PPP Φ_c and PHP Φ_h. One approach is to dissolve the hole, and the other is to approximate the PHP by a PPP with the same density. Without loss of generality, the user under consideration, i.e., the typical user, is assumed located at the origin. As defined in [4], a CU is in coverage when the SINR of its nearest BS corresponding to this CU is large enough. Therefore, the average coverage probability of CUs can be expressed as

$$P_{\mathrm{cov}}^{C} = \mathbb{E}\left[\mathbb{P}\left\{\mathrm{SINR}_k > \gamma_C\right\}\right], \quad (5)$$

where γ_C denotes the SINR threshold related to the CUs at the BS and

$$\begin{aligned} \mathbb{P}\left\{\mathrm{SINR}_k > \gamma_C\right\} &= \mathbb{P}\left\{\frac{P_c d_{k,o}^{-\alpha} \left|h_{k,o}\right|^2}{I_d + I_c + \sigma^2} > \gamma_C\right\} \\ &= \mathbb{P}\left\{\left|h_{k,o}\right|^2 > \frac{\gamma_C d_{k,o}^{\alpha}}{P_c}\left(I_d + I_c + \sigma^2\right)\right\} \\ &= \exp\left(-\frac{\gamma_C d_{k,o}^{\alpha} \sigma^2}{P_c}\right) \mathcal{L}_{I_d}(s)\, \mathcal{L}_{I_c}(s). \end{aligned} \quad (6)$$

By resorting to (2), we easily find that $\mathcal{L}_{I_d}(s)$ and $\mathcal{L}_{I_c}(s)$ denote the Laplace transforms of the random variables I_d and I_c evaluated at $s = \frac{\gamma_C d_{k,o}^{\alpha}}{P_c}$, respectively.

Similarly, the average coverage probability of DUs can be given by

$$P_{\mathrm{cov}}^{D} = \mathbb{E}\left[\mathbb{P}\left\{\mathrm{SINR}_j > \gamma_D\right\}\right], \quad (7)$$

where γ_D denotes the SINR threshold at the DRs and

$$\begin{aligned} \mathbb{P}\left\{\mathrm{SINR}_j > \gamma_D\right\} &= \mathbb{P}\left\{\frac{P_d d_{tr}^{-\alpha} \left|h_{j,j}\right|^2}{I_d' + I_c' + \sigma^2} > \gamma_D\right\} \\ &= \mathbb{P}\left\{\left|h_{j,j}\right|^2 > \frac{\gamma_D d_{tr}^{\alpha}}{P_d}\left(I_d' + I_c' + \sigma^2\right)\right\} \\ &= \exp\left(-\frac{\gamma_D d_{tr}^{\alpha} \sigma^2}{P_d}\right) \mathcal{L}_{I_d'}(s')\, \mathcal{L}_{I_c'}(s'). \end{aligned} \quad (8)$$

By resorting to (4), $\mathcal{L}_{I_d'}(s')$ and $\mathcal{L}_{I_c'}(s')$ denote the Laplace transforms of the random variables I_d' and I_c' evaluated at $s' = \frac{\gamma_D d_{tr}^{\alpha}}{P_d}$, respectively.

Actually, it is easy to obtain the Laplace transforms of these interferences in PPP just like [11]. However, when it comes to the mixed model of PHP and PPP, the problem becomes complicated, since there is still no accurate formula to get the Laplace transform for PHP. To address this, we take two methods in the following two subsections, where the expressions with subscripts 1 and 2 are used to denote the results of these two different approaches.

A. METHOD 1: DISSOLVING THE HOLE

In this subsection, the Theorem. 2 proposed in [13] will be employed to achieve the Laplace transform of interferences. Considering that the effect of the holes close to the typical node are much more important than the holes which are far away due to the pathloss, the hole which is closest to the typical node is dissolved while other holes are ignored. Therefore, this method will overestimate the interferences of the DUs, and hence leads to lower bounds on the Laplace transforms $\mathcal{L}_{I_d}(s)$ and $\mathcal{L}_{I_d'}(s')$. However, the local neighborhood around the typical node can be preserved while the far-field is simplified to attain tractability.

1) COVERAGE PROBABILITY ANALYSIS OF CELLULAR LINKS

In this part, we will analyze the coverage probability of cellular links and the typical node is BS. As shown in (6), it can be noted that the most important is to obtain the last two terms $\mathcal{L}_{I_d}(s)$ and $\mathcal{L}_{I_c}(s)$.

Firstly, we take effort to tackle with $\mathcal{L}_{I_d}(s)$, which is the Laplace transform of the D2D interferences from Φ_h to the BS. Notably, the Theorem. 2 in [13] cannot be used directly in

our considered scenario. Although the interferences characterized in [13] are analyzed for the typical node in the PHP, the typical node in this literature, however, is not BS. By contrast, in [20], the interferences for PHP are characterized at an arbitrary location by using the same technique as in [13]. Hence, the Lemma. 4 in [20] will be referred to.

Specifically, when the BS is set at the origin and the coordinate of the nearest hole center, i.e., the nearest CU, to the origin is $\mathbf{V_1}$, the formula (9) at the bottom of the page is obtained, where v_1 denotes $\|\mathbf{V_1}\|$ and $r_c = d_{k,o}$. In addition, the function $\hat{g}(v_1)$ can be expressed as

$$\hat{g}(v_1) = \begin{cases} \int_0^{D-v_1} \dfrac{2\pi\lambda_d' r}{1+\dfrac{r^a}{sP_d}} dr \\ \quad + \int_{D-v_1}^{D+v_1} \dfrac{2\lambda_d' r \arccos\left(\dfrac{r^2+{v_1}^2-D^2}{2v_1 r}\right)}{1+\dfrac{r^\alpha}{sP_d}} dr, v_1 \leqslant D; \\ \int_{v_1-D}^{v_1+D} \dfrac{2\lambda_d' r \arccos\left(\dfrac{r^2+{v_1}^2-D^2}{2v_1 r}\right)}{1+\dfrac{r^\alpha}{sP_d}} dr, v_1 > D. \end{cases} \tag{10}$$

Proof: See Appendix A. □

Secondly, after performing some mathematical analysis, $\mathcal{L}_{I_c}(s)$ can be obtained as

$$\mathcal{L}_{I_c}(s) = \exp\left[-\frac{2\pi^2\lambda_c}{\alpha\sin\left(2\pi/\alpha\right)}\gamma_C{}^{\frac{2}{\alpha}} r_c^2\right]. \tag{11}$$

By substituting (9) and (11) into (6), the coverage probability of cellular links can be represented as (12), shown at the bottom of the page, when $M > 1$, where $f_{r_c}(r_c) = 2r_c/R^2$ is the probability density function of r_c. The expression (12) is suitable for the non-orthogonal resource-sharing manner among CUs. When it comes to the orthogonal manner (i.e., $M = 1$, the inter-CUs interference $I_c = 0$, so $\mathcal{L}_{I_c}(s) = 1$), the coverage probability can be expressed as (13), shown at the bottom of the page.

2) COVERAGE PROBABILITY ANALYSIS OF D2D LINKS

In this part, the coverage probability of D2D links will be analyzed and the typical user in the origin can be any DR. Similarly, the last two terms $\mathcal{L}_{I_d'}(s')$ and $\mathcal{L}_{I_c'}(s')$ in (8) are the keys to the analysis.

Firstly, $\mathcal{L}_{I_d'}(s')$ is addressed. Considering that the typical user (i.e., j-th DR) is just the node in Φ_h, the Theorem.2 proposed in [13] can be used directly. The equation (14) can then be achieved when the j-th DR is at the origin and

$$\begin{cases} \mathcal{L}_{I_d}(s) > \mathcal{L}_{I_d,1}(s) = \exp\left[-\dfrac{2\pi^2\lambda_d'}{\alpha\sin\left(2\pi/\alpha\right)}\left(\dfrac{\gamma_C P_d}{P_c}\right)^{\frac{2}{\alpha}} r_c^2\right] \\ \qquad \times\left[\int_0^{r_c}\exp\left(\hat{g}(v_1)\right)\cdot\dfrac{2v_1}{R^2}dv_1 + \exp\left(\hat{g}(r_c)\right)\cdot\left(1-\dfrac{r_c^2}{R^2}\right)\right], \quad M>1; \\ \mathcal{L}_{I_d}(s) = \mathcal{L}_{I_d,1}(s) = \exp\left[-\dfrac{2\pi^2\lambda_d'}{\alpha\sin\left(2\pi/\alpha\right)}\left(\dfrac{\gamma_C P_d}{P_c}\right)^{\frac{2}{\alpha}} r_c^2\right]\times\exp\left(\hat{g}(r_c)\right), \quad M=1. \end{cases} \tag{9}$$

$$\begin{aligned} P_{\text{cov}}^C > P_{\text{cov},1}^C &= \mathbb{E}\left[\exp\left(-\frac{\gamma_C d_{k,o}^\alpha \sigma^2}{P_c}\right)\mathcal{L}_{I_d,1}(s)\,\mathcal{L}_{I_c}(s)\right] = \int_0^R \exp\left(-\frac{\gamma_C r_c^\alpha \sigma^2}{P_c}\right)\mathcal{L}_{I_d,1}(s)\,\mathcal{L}_{I_c}(s) f_{r_c}(r_c)\,dr_c \\ &= \int_0^R \exp\left(-\frac{\gamma_C r_c^\alpha \sigma^2}{P_c}\right)\exp\left[-\frac{2\pi^2\lambda_d'}{\alpha\sin\left(2\pi/\alpha\right)}\left(\frac{\gamma_C P_d}{P_c}\right)^{\frac{2}{\alpha}} r_c^2\right] \\ &\quad\times\left[\int_0^{r_c}\exp\left(\hat{g}(v_1)\right)\times\frac{2v_1}{R^2}dv_1 + \exp\left(\hat{g}(r_c)\right)\left(1-\frac{r_c^2}{R^2}\right)\right]\times\exp\left[-\frac{2\pi^2\lambda_c}{\alpha\sin\left(2\pi/\alpha\right)}(\gamma_C)^{\frac{2}{\alpha}} r_c^2\right]\times\frac{2r_c}{R^2}dr_c \end{aligned} \tag{12}$$

$$P_{\text{cov}}^C = P_{\text{cov},1}^C = \int_0^R \exp\left(-\frac{\gamma_C r_c^\alpha \sigma^2}{P_c}\right)\exp\left[-\frac{2\pi^2\lambda_d'}{\alpha\sin\left(2\pi/\alpha\right)}\left(\frac{\gamma_C P_d}{P_c}\right)^{\frac{2}{\alpha}} r_c^2\right]\exp\left(\hat{g}(r_c)\right)\times\frac{2r_c}{R^2}dr_c \tag{13}$$

$$\begin{aligned} \mathcal{L}_{I_d'}(s') \geqslant \mathcal{L}_{I_d',1}(s') &= \exp\left[-\frac{2\pi^2\lambda_d'}{\alpha\sin\left(2\pi/\alpha\right)}\gamma_D{}^{\frac{2}{\alpha}} d_{tr}^2\right]\times\int_D^\infty \exp\left(\hat{g}(v_2)\right) f_{\mathbf{V_2}}(v_2)dv_2 \\ &= \exp\left[-\frac{2\pi^2\lambda_d'}{\alpha\sin\left(2\pi/\alpha\right)}\gamma_D{}^{\frac{2}{\alpha}} d_{tr}^2\right]\times\int_D^\infty \exp\left(\hat{g}(v_2)\right)2\pi\lambda_c v_2\exp\left[-\pi\lambda_c\left(v_2^2-D^2\right)\right]dv_2 \end{aligned} \tag{14}$$

the coordinate of its nearest CU is $\mathbf{V_2}$. In (14), v_2 denotes $\|\mathbf{V_2}\|$ and $v_2 > D$. Moreover, the probability density function of v_2 is known as $f_{\mathbf{V_2}}(v_2) = 2\pi\lambda_c v_2 exp\left[-\pi\lambda_c\left(v_2^2 - D^2\right)\right]$ from [13].

Secondly, using the similar manipulation of deriving the first term at the right of the equal sign when $M > 1$ in (9), $\mathcal{L}_{I_c'}(s')$ can be acquired with D being the lower limit of the integral as

$$\mathcal{L}_{I_c'}(s') = \exp\left(-2\pi\lambda_c \int_D^{\infty} \frac{s' P_c t^{-\alpha+1}}{1 + s' P_c t^{-\alpha}} dt\right), \quad (15)$$

where $t = d_{k,j}$.

By substituting (14) and (15) into (8), the D2D links' coverage probability can be denoted as (16) at the bottom of the page. Obviously, with the above method, the expressions of user coverage probabilities $P_{\text{cov},1}^C$ and $P_{\text{cov},1}^D$ are both very complex due to containing multiple integrals, which makes it difficult to perform further analysis. Hence, in order to gain the insights deeply, we will devote to achieve the coverage probabilities in a simple way.

B. METHOD 2: APPROXIMATING THE PHP THROUGH A THINNED PPP

In this subsection, a simple method is adopted to get the user coverage probabilities. When it comes to $\mathcal{L}_{I_d}(s)$ and $\mathcal{L}_{I_d'}(s')$, we adopt first-order statistic approximation to approximate the PHP Φ_h by a PPP $\hat{\Phi}_d$ with the same density, in which the baseline PPP Φ_d is independently thinned. That is, the resulting density of PPP $\hat{\Phi}_d$ is the same as the density of PHP Φ_h i.e., $\lambda_d = \lambda_d' exp\left(-\lambda_c \pi D^2\right)$ [5].

1) COVERAGE PROBABILITY ANALYSIS OF CELLULAR LINKS

The distribution and density of DUs will evidently not affect $\mathcal{L}_{I_c}(s)$, which still follows (11). Nevertheless, for $\mathcal{L}_{I_d}(s)$, it can be approximated as

$$\mathcal{L}_{I_d}(s) \approx \mathcal{L}_{I_d,2}(s) = \exp\left[-\frac{2\pi^2\lambda_d}{\alpha \sin\left(2\pi/\alpha\right)}\left(\frac{\gamma_C P_d}{P_c}\right)^{\frac{2}{\alpha}} r_c^2\right]. \quad (17)$$

By substituting (17) and (11) into (6), the cellular links' coverage probability can be approximatively expressed as

$$P_{\text{cov}}^C \approx P_{\text{cov},2}^C = \mathbb{E}\left[\exp\left(-\frac{\gamma_C d_{k,o}^{\alpha}\sigma^2}{P_c}\right)\mathcal{L}_{I_d,2}(s)\,\mathcal{L}_{I_c}(s)\right]$$
$$= \int_0^R \exp\left(-\frac{\gamma_C r_c^{\alpha}\sigma^2}{P_c}\right) \times \mathcal{L}_{I_d,2}(s)\,\mathcal{L}_{I_c}(s) f_{r_c}(r_c)\, dr_c$$
$$= \int_0^R e^{-a r_c^{\alpha} - b r_c^2 - c r_c^2} \frac{2r_c}{R^2} dr_c, \quad (18)$$

where $a = \frac{\gamma_C \sigma^2}{P_c}$, $b = \frac{2\pi^2\lambda_d}{\alpha \sin(2\pi/\alpha)}\left(\frac{\gamma_C P_d}{P_c}\right)^{\frac{2}{\alpha}}$, and $c = \frac{2\pi^2\lambda_c}{\alpha \sin(2\pi/\alpha)}(\gamma_C)^{\frac{2}{\alpha}}$.

Since this equation involves the integral formula, which prevents us to obtain deep insights, we can take the specific α into account to simplify it. Without loss of generality, similar to [11], the following two special cases are investigated.

Case 1: $\alpha = 4$ with noise (i.e., $\sigma^2 \neq 0$). In the presence of noise, by substituting $\alpha = 4$ into (18), the new expression can be derived as

$$P_{\text{cov}}^C \approx P_{\text{cov},2}^C$$
$$= \frac{1}{R^2}\sqrt{\frac{\pi}{4a}} \exp\left[\frac{(b+c)^2}{4a}\right]$$
$$\times \left[\phi\left((b+c)\sqrt{\frac{1}{4a}} + R^2\sqrt{a}\right) - \phi\left((b+c)\sqrt{\frac{1}{4a}}\right)\right], \quad (19)$$

where $\phi(x) = \frac{1}{\sqrt{\pi}}\int_0^{x^2} \frac{e^{-t}}{\sqrt{t}} dt$ [25].

Case 2: $\alpha = 4$ without noise (i.e., $\sigma^2 = 0$). By substituting $\alpha = 4$ and $\sigma^2 = 0$ into (18), the closed-form expression of cellular links' coverage probability can be simplified as

$$P_{\text{cov}}^C \approx P_{\text{cov},2}^C$$
$$= \frac{1 - \exp\left[-\frac{\pi^2 R^2\sqrt{\gamma_C}}{2}\left(\lambda_d\sqrt{\frac{P_d}{P_c}} + \lambda_c\right)\right]}{\frac{\pi^2 R^2\sqrt{\gamma_C}}{2}\left(\lambda_d\sqrt{\frac{P_d}{P_c}} + \lambda_c\right)}. \quad (20)$$

Similar to the part III-A1, considering our proposed scenario, the above equation is suitable for the non-orthogonal resource-sharing manner among CUs. When it comes to that CUs share the uplink spectrum resources in an orthogonal manner (i.e., $M = 1$, the inter-CUs interference $I_c = 0$), and $\lambda_d = \lambda_d' exp\left(-\frac{1}{\pi R^2}\pi D^2\right)$ for $\lambda_c = \frac{1}{\pi R^2}$, (20) can then be written as

$$P_{\text{cov}}^C \approx P_{\text{cov},2}^C = \frac{1 - \exp\left[-\frac{\pi^2 R^2}{2}\lambda_d' \exp\left(-\frac{D^2}{R^2}\right)\sqrt{\frac{\gamma_C P_d}{P_c}}\right]}{\frac{\pi^2 R^2}{2}\lambda_d' \exp\left(-\frac{D^2}{R^2}\right)\left(\sqrt{\frac{\gamma_C P_d}{P_c}}\right)}. \quad (21)$$

It is worth noting that (13) and (21) can be widely used in simplified models for PHP-based cellular systems, where each CU possesses an individual uplink spectrum shared with several D2D pairs.

$$P_{\text{cov}}^D \geqslant P_{\text{cov},1}^D = \mathbb{E}\left[\exp\left(-\frac{\gamma_D d_{tr}^{\alpha}\sigma^2}{P_d}\right)\mathcal{L}_{I_d',1}(s')\,\mathcal{L}_{I_c'}(s')\right] = \exp\left(-\frac{\gamma_D d_{tr}^{\alpha}\sigma^2}{P_d}\right) \times \exp\left[-\frac{2\pi^2\lambda_d'}{\alpha \sin\left(2\pi/\alpha\right)}\gamma_D^{\frac{2}{\alpha}} d_{tr}^2\right]$$
$$\times \int_D^{\infty} \exp\left(\hat{g}(v_2)\right) 2\pi\lambda_c v_2 \times \exp\left[-\pi\lambda_c(v_2^2 - D^2)\right] dv_2 \times \exp\left(-2\pi\lambda_c \int_D^{\infty} \frac{s' P_c t^{-\alpha+1}}{1 + s' P_c t^{-\alpha}} dt\right) \quad (16)$$

2) COVERAGE PROBABILITY ANALYSIS OF D2D LINKS

Similarly, since the distribution and density of DUs will not affect $\mathcal{L}_{I_c'}(s')$, $\mathcal{L}_{I_c'}(s')$ still follows (15). Meanwhile, $\mathcal{L}_{I_d'}(s')$ can be approximated as

$$\mathcal{L}_{I_d'}(s') \approx \mathcal{L}_{I_d',2}(s') = \exp\left[-\frac{2\pi^2\lambda_d}{\alpha \sin\left(2\pi/\alpha\right)}\gamma_D^{\frac{2}{\alpha}} d_{tr}^2\right]. \quad (22)$$

By substituting (22) and (15) into (8), the D2D links' coverage probability can be given by

$$P_{\text{cov}}^D \approx P_{\text{cov},2}^D = \exp\left[-\frac{\gamma_D d_{tr}^{\alpha}\sigma^2}{P_d} - \frac{2\pi^2\lambda_d}{\alpha \sin\left(2\pi/\alpha\right)}\gamma_D^{\frac{2}{\alpha}} d_{tr}^2 - 2\pi\lambda_c \int_D^{\infty} \frac{s' P_c t^{-\alpha+1}}{1 + s' P_c t^{-\alpha}} dt\right], \quad (23)$$

which is also difficult to simplify due to the integral operation. Therefore, using the same way as the last part, the following two special cases are investigated.

Case 1: $\alpha = 4$ with noise (i.e., $\sigma^2 \neq 0$). By substituting $\alpha = 4$ into (23), the expression of the D2D links' coverage probability can be obtained as (24) at the bottom of the page.

Case 2: $\alpha = 4$ without noise (i.e., $\sigma^2 = 0$). Since the impact of noise is ignored here, the expression for coverage probability of D2D links can be simplified as (25), shown at the bottom of the page, by substituting $\alpha = 4$ and $\sigma^2 = 0$ into (23).

Notably, the results of above two cases are both different from the results in [11], since the interferences from DUs and CUs are totally different from [11]. Now, the expressions of the coverage probabilities for users have been derived by the above two methods. Besides, the first method can capture the local neighborhood around the typical node accurately while simplifying the far-field to attain tractability. Nevertheless, the expressions obtained by the first method contain multiple integrals, which makes further analysis difficult. More importantly, the closed expressions of user coverage probabilities are obtained through the second method, and it is conducive to do comprehensive network performance evaluation and further analysis. In the following, the sum data rate of the networks will be analyzed through the second method.

IV. ANALYSIS AND OPTIMIZATION OF SUM DATA RATE

Considering the two approaches in the previous section, the results of the first method contain multiple integrals and thus are hard to simplify, while the second method is easier to expand for further analysis. Therefore, in this section, the second method is involved to achieve the ergodic data rates of cellular links and D2D links, as well as the sum data rate of the entire networks.

As discussed in [11], the ergodic data rate of cellular links can be given by

$$\bar{R}_C = \frac{2}{n \ln 2}\left[\frac{\pi}{2} - \text{ci}(n)\sin(n) + \text{si}(n)\cos(n)\right], \quad (26)$$

where $n = \frac{\pi^2 R^2}{2}\left(\lambda_d\sqrt{\frac{P_d}{P_c}} + \lambda_c\right)$, $\text{ci}(x) = -\int_x^{\infty}\frac{\cos(t)}{t}dt$ and $\text{si}(x) = -\int_x^{\infty}\frac{\sin(t)}{t}dt$.

Similarly, the D2D links' ergodic data rate can be represented as (27) at the bottom of the page.

To describe the performance improvement brought by active DUs in the networks, the notion of "data rate increment" is utilized here as in [11]. Specifically, the data rate increment in the investigated networks can be defined as

$$\Delta\bar{R} = \bar{R}_D - \bar{R}_C. \quad (28)$$

Next, we try to achieve the sum data rate of the entire networks. The sum data rate of D2D links can be given by

$$R_D = \mathbb{E}\left[\sum_{j=1}^{N}\log_2\left(1 + \text{SINR}_j\right)\right] = \lambda_d \pi R^2 \cdot \bar{R}_D, \quad (29)$$

$$P_{\text{cov}}^D \approx P_{\text{cov},2}^D = \exp\left(-\frac{\gamma_D d_{tr}^4\sigma^2}{P_d} - \frac{\pi^2\lambda_d}{2}\sqrt{\gamma_D} d_{tr}^2 - 2\pi\lambda_c\int_D^{\infty}\frac{s' P_c t^{-3}}{1 + s' P_c t^{-4}}dt\right)$$
$$= \exp\left[-\frac{\gamma_D d_{tr}^4\sigma^2}{P_d} - \frac{\pi^2\lambda_d' \exp\left(-\lambda_c\pi D^2\right)}{2}\sqrt{\gamma_D} d_{tr}^2 - \pi\lambda_c d_{tr}^2\sqrt{\frac{\gamma_D P_c}{P_d}}\arctan\frac{d_{tr}^2\sqrt{\frac{\gamma_D P_c}{P_d}}}{D^2}\right] \quad (24)$$

$$P_{\text{cov}}^D \approx P_{\text{cov},2}^D = \exp\left(-\frac{\pi^2\lambda_d}{2}\sqrt{\gamma_D} d_{tr}^2 - 2\pi\lambda_c\int_D^{\infty}\frac{s' P_c t^{-3}}{1 + s' P_c t^{-4}}dt\right)$$
$$= \exp\left[-\frac{\pi^2\lambda_d' \exp\left(-\lambda_c\pi D^2\right)}{2}\sqrt{\gamma_D} d_{tr}^2 - \pi\lambda_c d_{tr}^2\sqrt{\frac{\gamma_D P_c}{P_d}}\arctan\frac{d_{tr}^2\sqrt{\frac{\gamma_D P_c}{P_d}}}{D^2}\right] \quad (25)$$

$$\bar{R}_D = \frac{1}{\ln 2}\int_0^{\infty}\frac{\exp\left[-\frac{\pi^2\lambda_d' \exp\left(-\lambda_c\pi D^2\right)}{2}\sqrt{\gamma_D} d_{tr}^2\right]}{1 + \gamma_D} \times \exp\left(-\pi\lambda_c d_{tr}^2\sqrt{\frac{\gamma_D P_c}{P_d}}\arctan\frac{d_{tr}^2\sqrt{\frac{\gamma_D P_c}{P_d}}}{D^2}\right) d\gamma_D \quad (27)$$

and the sum data rate of cellular links can be similarly given by

$$R_C = \lambda_c \pi R^2 \cdot \bar{R}_C. \tag{30}$$

Then, the sum data rate of the proposed underlying networks can totally be expressed as

$$\begin{aligned} R_{sum} &= R_D + R_C = \lambda_d \pi R^2 \cdot \bar{R}_D + \lambda_c \pi R^2 \cdot \bar{R}_C \\ &= \lambda'_d \exp\left(-\lambda_c \pi D^2\right) \pi R^2 \cdot \bar{R}_D + \lambda_c \pi R^2 \cdot \bar{R}_C. \end{aligned} \tag{31}$$

By substituting (26) and (27) into (31), it can be found that the sum data rate is the function of the DUs' density λ'_d. With the increase of λ'_d, there will be more DUs leading to the improvement of the sum data rate. However, at the same time, more DUs will produce more serious interferences in the networks, which will result in the decreasing of the ergodic data rates of DUs and CUs. Therefore, there exists a reasonable DUs' density in terms of maximizing the sum data rate. Based on the discussion above, now we are committed to getting the optimal DUs' density λ'_d, which is helpful to design the D2D-aided cellular networks. The optimal DUs' density λ'_d can be obtained by maximizing the sum data rate under the constraints of guaranteeing the QoS of cellular and D2D links. The optimization problem can be formulated as

$$\begin{aligned} P1: \ & \max_{\lambda'_d} \ R_{sum} \\ & \text{s.t. } \theta_c < P_{\text{cov}}^C \leqslant 1, \\ & \quad \theta_d < P_{\text{cov}}^D \leqslant 1, \end{aligned} \tag{32}$$

where θ_c and θ_d represent the minimum coverage probability of CUs and DUs, respectively.

According to the optimization problem given in (32), the DUs' density λ'_d can be upper-bounded as

$$\begin{cases} \lambda'_d < \dfrac{\lambda_c - 2\theta_c W\left(-\exp\left(-1/\theta_c\right)/\theta_c\right) - 2}{\pi^2 R^2 \theta_c \sqrt{\gamma_C P_d / P_c}}, \\ \lambda'_d < \dfrac{-2\left(\ln\left(\theta_d\right) + \pi \lambda_c d_{tr}^2 \sqrt{\dfrac{\gamma_D P_c}{P_d}} \arctan \dfrac{d_{tr}^2 \sqrt{\dfrac{\gamma_D P_c}{P_d}}}{D^2}\right)}{\pi^2 \exp\left(-\lambda_c \pi D^2\right) \sqrt{\gamma_D} d_{tr}^2}, \end{cases} \tag{33}$$

where $W(\cdot)$ represents the Lambert W function, which is the inverse function of $f(W) = We^W$. Note that the optimization problem P1 is hard to obtain the optimal solution λ'_d in closed form due to R_{sum} containing multiple integrals. Therefore, we intend to find the optimal λ'_d by numerical evaluation, and the simulations as well as the analysis are provided in the following section.

V. NUMERICAL RESULT

In this section, the results of both the two methods will be compared with the simulation results (which are the average coverage probabilities of users through 20000 rounds of the simulation) for verifying the theoretical correctness and the completeness of our work. Also, the numerical results will be presented to evaluate the impacts of different system parameters on network performance. Specifically, the impacts of the density of DUs λ'_d, the transmit power ratio between CUs and DTs P_c/P_d, and the size of the warning radius D on the data rate increment are analyzed. Moreover, the influences of λ'_d, D and the number of CUs on the sum data rate are also evaluated. Without loss of generality, the area in each experiment is assumed to be a circle with radius R, in which the BS is deployed in the origin. Besides, all $M = \lambda_c \pi R^2$ CUs and $K = \lambda'_d \pi R^2$ DUs are spatially distributed according to the PPP Φ_c and the PPP Φ_d, respectively. Thus, the locations of the $N = \lambda'_d \exp\left(-\lambda_c \pi D^2\right) \pi R^2$ active DUs outside the holes are spatially distributed according to the PHP $\Phi_h\left(\lambda_c, \lambda'_d, D\right)$. Simulation parameters are given in Table 1, which refer to the related literatures [20], [26], [27].

TABLE 1. Simulation parameters.

Simulation Parameters	Value
Cell radius R	500 m
Transmit power for CUs P_c	100 mW
Transmit power for DTs P_d	1 mW
Pathloss exponent α	4
The number of CUs M	1, 3, 5, 10

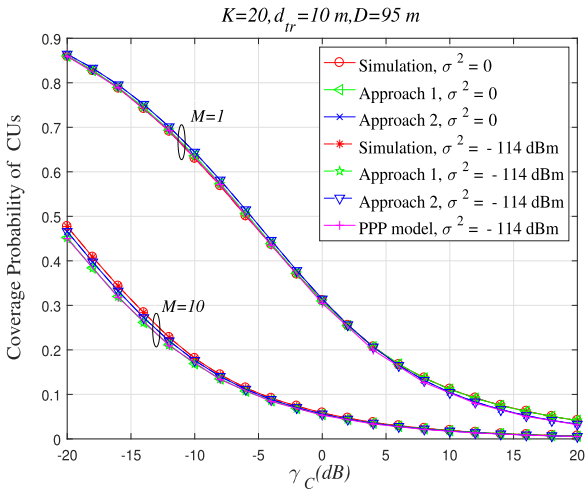

FIGURE 2. Coverage probability of CUs when $M = 1$ and 10.

Fig. 2 and Fig. 3 illustrate the coverage probabilities of cellular links and D2D links with different M, respectively, where $M = 1$ means the orthogonal resource-sharing manner among CUs. As shown in the two diagrams, the analytical results obtained by two methods based on PHP model both coincide with the simulations, while the results based on PPP model in [11] cannot reflect the true state compared to the simulations in terms of DUs' coverage probability. This means PHP model has a better performance than PPP model due to considering the exclusion between DUs and CUs. Thus, the numerical expressions based on PHP model can be well utilized to achieve the corresponding coverage probability in the proposed system. It can also be seen that increasing M will lead to the reduction of the coverage probability

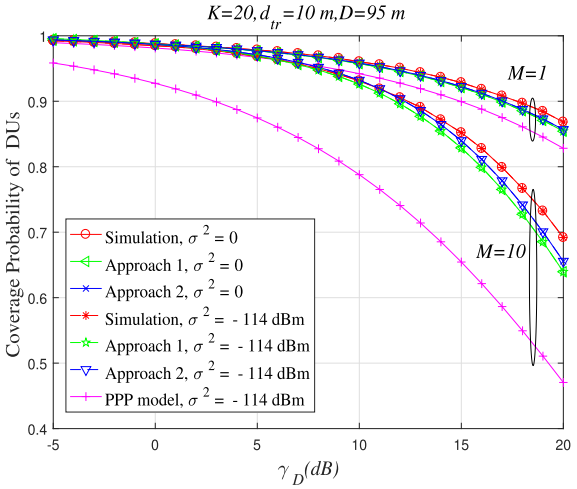

FIGURE 3. Coverage probability of DUs when $M = 1$ and 10.

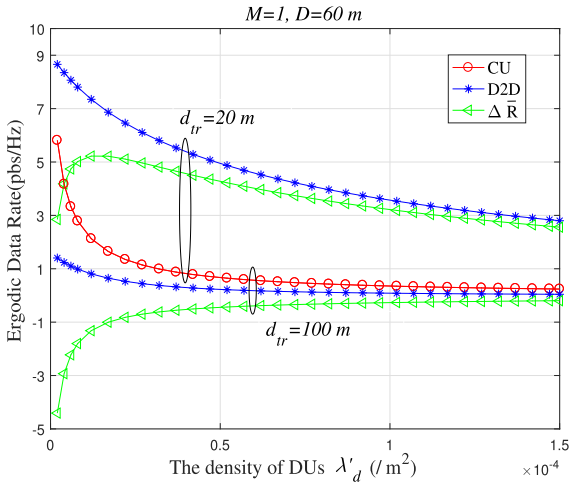

FIGURE 4. Ergodic data rate and data rate increment with increasing λ'_d for different d_{tr}.

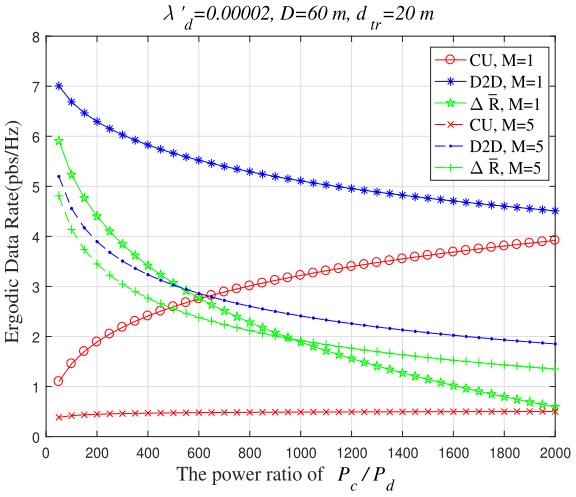

FIGURE 5. Ergodic data rate and data rate increment with increasing power ratio between P_c and P_d.

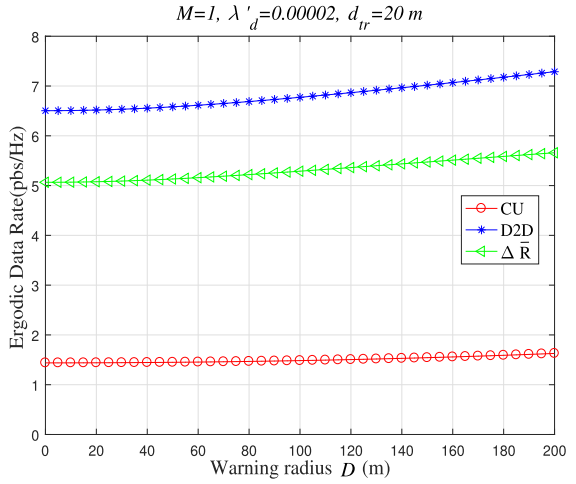

FIGURE 6. Ergodic data rate increases as D increases.

due to severer interference in the system. In addition, both figures show that the coverage probability decreases when the SINR threshold increases. It is worth noting that the noise has little effect on the coverage probability, which means the expressions without noise can be well employed for the subsequent experiments. Moreover, considering that the second method is easier for further analyses than the first one, in the following, it is used to analyze data rate increment and sum data rate.

Fig. 4 shows the impacts of the original DUs' density λ'_d on the ergodic data rates of users and data rate increment $\Delta\bar{R}$ when d_{tr} equals 20 m and 100 m. As we can see, not all the settings can guarantee that the network performance will be improved by activating D2D links. In details, $\Delta\bar{R}$ is positive when $d_{tr} = 20$ m, indicating that adding D2D communication has a positive contribution to the sum data rate of the system. When $d_{tr} = 100$ m, $\Delta\bar{R}$ is negative, meaning that the sum data rate may be degraded. Besides, the ergodic data rates of CUs and DUs decrease as λ'_d increases due to the severe interferences, and the different decreasing speeds cause the data rate increment to increase first and then decrease when $d_{tr} = 20$ m. This suggests only proper D2D configurations will promote network performance.

In Fig. 5, the effects of the power ratio between P_c and P_d on user ergodic data rates are presented for different numbers of CUs M. When other parameters are fixed (such as the density of DUs, the warning radius D, the power of CUs P_c and so on), it can be seen from the figure that with the power of DUs P_d decreasing, the ergodic data rate of CUs increases, while the ergodic data rate of DUs decreases and the data rate increment drops significantly. This means the contribution brought by D2D communication to the sum data rate of the networks decreases. Therefore, when considering a real network scenario, we should balance the ergodic data rate of CUs and the sum data rate of the D2D-aided cellular networks. In other words, the transmitter power of DUs is

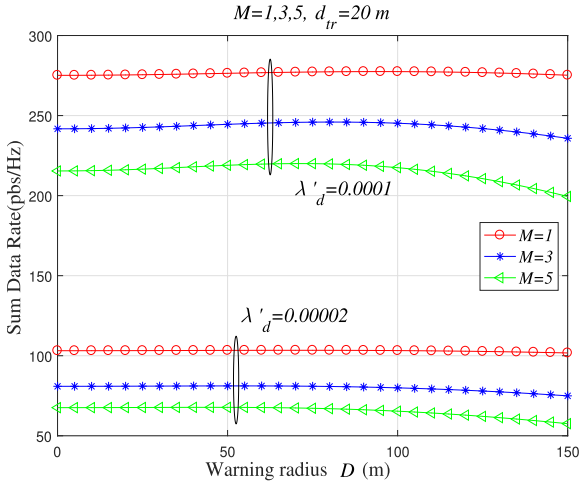

FIGURE 7. Curves of sum data rate as warning radius D increases.

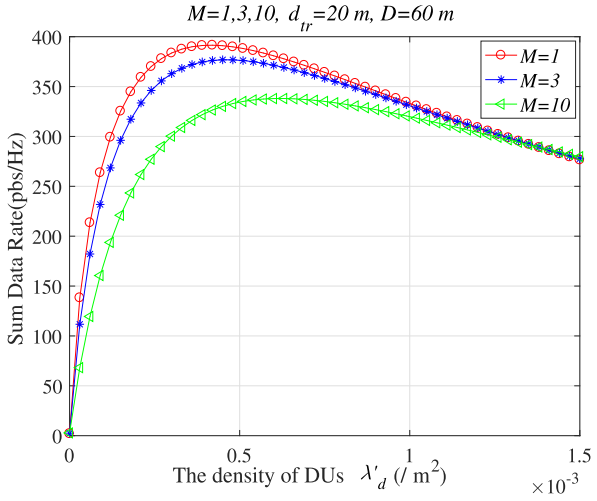

FIGURE 8. Curves of sum data rate as the density of DUs λ'_d increases.

easier to derive when the data rate threshold of CUs and other parameters are fixed. Besides, it can also be seen that when the number of CUs increases, the ergodic data rates of CUs and DUs both drop a lot, and the larger M is, the more slightly the curve of the ergodic data rate of CUs increases even though the power ratio increases.

Fig. 6 depicts the ergodic data rate and data rate increment as functions of the warning radius D. It shows the ergodic data rate of DUs increases obviously as D increases. This is because the distances from CUs to active DRs increase and the density of DUs decreases, which leads to the interferences reducing. Meanwhile, the larger D is, the larger ergodic data rate of CUs is, due to the less active DUs. However, since the transmit power levels of DTs are always low, the impact of D on the CUs' ergodic data rate is slight. As a result, the data rate increment increases.

In Fig. 7, we illustrate the relationship between the warning radius D and the sum data rate R_{sum} with different M and λ'_d. From the figure, we can see that when the density of D2D pairs equals to 0.00002, each curve stays flat at the beginning, and then decreases as D continues to increase. This is because with the increases of D at the beginning, the density of active D2D pairs decreases for $\lambda_d = \lambda'_d \exp\left(-\lambda_c \pi D^2\right)$, while the ergodic data rate of DUs continues to increases known from the Fig. 6. Thus, although increasing D causes less active D2D pairs in the networks, it can protect the QoS of users and also keep the sum data rate stay a steady state. However, the warning radius cannot be too large. Since D continues to increase, the D^2 increases faster than before and the number of active DUs decreases quickly. The effect of reduction of the number of active DUs is currently more defining. When the density of DUs increases to 0.0001, the sum data rate increases a lot than the low density of DUs. Therefore, we can choose a suitable D according to the QoS of CUs and DUs, which can help keep the sum data rate stable. In addition, when the number of CUs (i.e., M) increases, the sum data rate of the networks decreases due to the enlarged mutual interferences between users.

Finally, Fig. 8 represents the impacts of the original DUs' density λ'_d on the sum data rate with different M. It can be seen from the figure that as λ'_d just rises from zero, the sum data rate increases significantly. Then, it gradually reaches a maximum value before slowly decreases. The reason is, at the beginning, DUs' joining the networks can significantly improve the network performance. However, when λ'_d continues to increase, the interference situation in the networks becomes worse and the data rate increment $\Delta\bar{R}$ decreases as shown in Fig. 4. Those eventually result in that the sum data rate declines. Similar to Fig. 7, Fig. 8 also indicates that when the number of CUs increases, the sum data rate of the networks decreases, due to the interferences caused by CUs being more serious. Therefore, the optimal density of DUs can be obtained through the numerical evaluation, which is helpful for the mode selection of users.

VI. CONCLUSION

In this paper, we have proposed a new analysis framework for the D2D-aided underlaying uplink cellular networks with the PPP-and-PHP hybrid model, where DUs can reuse the same licensed uplink spectrum with CUs. The manners of non-orthogonal and orthogonal frequency division multiplexing for CUs are both investigated. To analyze the coverage probabilities of CUs and DUs, two methods are adopted, before one of them is utilized to obtain expressions of the users' ergodic data rate and the sum data rate. With these expressions, it can be more intuitional to analyze the impacts of the key parameters on users' coverage probability and sum data rate, which is not easy to achieve by Monte Carlo simulations. Numerical results show that the proposed model is more reasonable than others, and thus may be practical in designing a general network. For the future work, we will focus on the performance analysis for the more complex network model, including the downlink cellular networks.

APPENDIX A
PROOF OF $\mathcal{L}_{I_d}(s)$

When we consider the only one hole formed by the CU which is closest to the BS, the Laplace transform of D2D interferences conditioned on the distance v_1 is represented as

$$\begin{aligned}
&\mathcal{L}_{I_d,1|v_1}(s)\\
&= \mathbb{E}\left[\exp\left(-s\sum_{i'\in\Phi_d/\mathbf{b}(\mathbf{V}_1,D)} P_d d_{i',o}^{-\alpha}\left|h_{i',o}\right|^2\right)\right]\\
&\overset{(a)}{=} \mathbb{E}_{\Phi_d}\left[\prod_{i'\in\Phi_d/\mathbf{b}(\mathbf{V}_1,D)} \mathbb{E}_{h_{i',o}}\left[\exp\left(-sP_d d_{i',o}^{-\alpha}\left|h_{i',o}\right|^2\right)\right]\right]\\
&\overset{(b)}{=} \mathbb{E}_{\Phi_d}\left[\prod_{i'\in\Phi_d/\mathbf{b}(\mathbf{V}_1,D)} \frac{1}{1+sP_d d_{i',o}^{-\alpha}}\right]\\
&\overset{(c)}{=} \exp\left[-\lambda_d'\int_{\mathbb{R}^2/\mathbf{b}(\mathbf{V}_1,D)} \frac{1}{1+\frac{x^\alpha}{sP_d}}dx\right]\\
&= \exp\left[-\lambda_d'\left(\int_{\mathbb{R}^2} \frac{1}{1+\frac{x^\alpha}{sP_d}}dx - \int_{\mathbf{b}(\mathbf{V}_1,D)} \frac{1}{1+\frac{x^\alpha}{sP_d}}dx\right)\right]\\
&\overset{(d)}{=} \exp\left[-2\pi\lambda_d'\int_0^\infty \frac{x}{1+\frac{x^\alpha}{sP_d}}dx - \lambda_d'\int_{\mathbf{b}(\mathbf{V}_1,D)} \frac{1}{1+\frac{x^\alpha}{sP_d}}dx\right]\\
&= \exp\left[-2\pi\lambda_d'\int_0^\infty \frac{sP_d x^{-\alpha+1}}{1+sP_d x^{-\alpha}}dx - \lambda_d'\int_{\mathbf{b}(\mathbf{V}_1,D)} \frac{1}{1+\frac{x^\alpha}{sP_d}}dx\right]\\
&\overset{(e)}{=} \exp\left[-\frac{2\pi^2\lambda_d'}{\alpha\sin\left(2\pi/\alpha\right)}\left(\frac{\gamma_C P_d}{P_c}\right)^{\frac{2}{\alpha}} d_{k,o}^2\right]\times\exp\left(\hat{g}\left(v_1\right)\right)
\end{aligned} \tag{34}$$

where $\mathbf{b}(\mathbf{V}_1, D)$ represents the exclusion zone centered at $\mathbf{V}_1$ with radius D. Besides, x represents the distance $d_{i',o}$ between the i'-th DT, which belongs to Φ_d and is not in the area $\mathbf{b}(\mathbf{V}_1, D)$, and the BS. Moreover, $h_{i',o}$ denotes the channel coefficient between them. In this equation, the step (a) follows that the channel coefficients are independently identically distribution. The step (b) obeys that the square of the Rayleigh fading channel coefficient is exponential distribution and then $e^{-\delta A} = \frac{1}{1+A}$ when $\delta \to \exp(1)$. The step (c) follows the probability generating functional of a PPP, i.e., $\mathbb{E}\left[\prod_{i\in\Phi} f(x)\right] = \exp\left[-\lambda\int_{\mathbb{R}^2}(1-f(x))\,dx\right]$, and the step (d) converts the integral from Cartesian to polar coordinates. Furthermore, the first term after the step (e) can refer to the [25 Eq. 3.241.4], and the second term can refer to the Lemma.4 in [20].

Therefore, when $M > 1$, $\mathcal{L}_{I_d,1}(s)$ can be represented by

$$\begin{aligned}
\mathcal{L}_{I_d,1}(s) &= \int_0^{r_c} \mathcal{L}_{I_d,1|v_1}(s) f_{\mathbf{V_1}}(v_1)\,dv_1\\
&= \exp\left[-\frac{2\pi^2\lambda_d'}{\alpha\sin\left(2\pi/\alpha\right)}\left(\frac{\gamma_C P_d}{P_c}\right)^{\frac{2}{\alpha}} r_c^2\right]\\
&\quad\times\left[\int_0^{r_c}\exp\left(\hat{g}\left(v_1\right)\right)\cdot\frac{2v_1}{R^2}dv_1 + \exp\left(\hat{g}\left(r_c\right)\right)\right.\\
&\quad\left.\cdot\left(1-\frac{r_c^2}{R^2}\right)\right],
\end{aligned} \tag{35}$$

where $r_c = d_{k,o}$ and $f_{\mathbf{V_1}}(v_1)$ is the probability density function (PDF) of v_1, which can be given by

$$f_{\mathbf{V_1}}(v_1) = \begin{cases} \dfrac{2v_1}{R^2}, & v_1 < r_c;\\ 1-\dfrac{r_c^2}{R^2}, & v_1 = r_c. \end{cases} \tag{36}$$

The reason for which (36) is tenable is explained as follows. When $v_1 < r_c$, the PDF of the distance between the nearest hole center and the origin follows $f_{\mathbf{V_1}}(v_1) = 2v_1/R^2$. However, when $v_1 = r_c$, the nearest CU to the origin is just the analyzed CU itself. It means the probability of no CUs being in the circle with the distance r_c from the origin is $\left(\pi R^2 - \pi r_c^2\right)/\left(\pi R^2\right) = 1 - \frac{r_c^2}{R^2}$. On the other hand, when $M = 1$, there are only one hole formed by the analyzed CU.Therefore, the probability of $v_1 = r_c$ equals one, which results in $\mathcal{L}_{I_d,1}(s)$ being equivalent to $\mathcal{L}_{I_d,1|v_1=r_c}(s)$.

REFERENCES

[1] X. Lin, J. Andrews, A. Ghosh, and R. Ratasuk, "An overview of 3GPP device-to-device proximity services," *IEEE Commun. Mag.*, vol. 52, no. 4, pp. 40–48, Apr. 2014.

[2] S. W. H. Shah, M. M. U. Rahman, A. N. Mian, A. Imran, S. Mumtaz, and O. A. Dobre, "On the impact of mode selection on effective capacity of Device-to-Device communication," *IEEE Wireless Commun. Lett.*, vol. 8, no. 3, pp. 945–948, Jun. 2019.

[3] K. M. S. Huq, S. Mumtaz, J. Rodriguez, P. Marques, B. Okyere, and V. Frascolla, "Enhanced C-RAN using D2D network," *IEEE Commun. Mag.*, vol. 55, no. 3, pp. 100–107, Mar. 2017.

[4] J. G. Andrews, F. Baccelli, and R. K. Ganti, "A tractable approach to coverage and rate in cellular networks," *IEEE Trans. Commun.*, vol. 59, no. 11, pp. 3122–3134, Nov. 2011.

[5] M. Haenggi, *Stochastic Geometry for Wireless Networks*. Cambridge, U.K.: Cambridge Univ. Press, 2012.

[6] Y. S. Soh, T. Q. S. Quek, M. Kountouris, and H. Shin, "Energy efficient heterogeneous cellular networks," *IEEE J. Sel. Areas Commun.*, vol. 31, no. 5, pp. 840–850, May 2013.

[7] H. A. Mustafa, M. Z. Shakir, M. A. Imran, A. Imran, and R. Tafazolli, "Coverage gain and device-to-device user density: Stochastic geometry modeling and analysis," *IEEE Commun. Lett.*, vol. 19, no. 10, pp. 1742–1745, Oct. 2015.

[8] C.-H. Lee and M. Haenggi, "Interference and outage in Poisson cognitive networks," *IEEE Trans. Wireless Commun.*, vol. 11, no. 4, pp. 1392–1401, Apr. 2012.

[9] N. Haider, A. Ali, Y. He, and E. Dutkiewicz, "Performance analysis of full duplex D2D in opportunistic spectrum access," in *Proc. 18th Int. Symp. Commun. Inf. Technol. (ISCIT)*, Bangkok, Thailand, Sep. 2018, pp. 32–37.

[10] C. Galiotto, N. K. Pratas, L. Doyle, and N. Marchetti, "Effect of LOS/NLOS propagation on 5G ultra-dense networks," *Comput. Netw.*, vol. 120, pp. 126–140, Jun. 2017.

[11] J. Sun, T. Liu, X. Wang, C. Xing, H. Xiao, A. V. Vasilakos, and Z. Zhang, "Optimal mode selection with uplink data rate maximization for D2D-aided underlaying cellular networks," *IEEE Access*, vol. 4, pp. 8844–8856, 2016.

[12] Y. PanZiyu and H. BaoZiyong, "Approximate coverage analysis of heterogeneous cellular networks modeled by Poisson hole process," in *Proc. IEEE 18th Int. Conf. Commun. Technol. (ICCT)*, Chongqing, China, Oct. 2018, pp. 424–427.

[13] Z. Yazdanshenasan, H. S. Dhillon, M. Afshang, and P. H. J. Chong, "Poisson hole process: Theory and applications to wireless networks," *IEEE Trans. Wireless Commun.*, vol. 15, no. 11, pp. 7531–7546, Nov. 2016.
[14] M. A. Kishk and H. S. Dhillon, "Tight lower bounds on the contact distance distribution in Poisson hole process," *IEEE Wireless Commun. Lett.*, vol. 6, no. 4, pp. 454–457, Aug. 2017.
[15] I. Flint, H.-B. Kong, N. Privault, P. Wang, and D. Niyato, "Analysis of heterogeneous wireless networks using Poisson hard-core hole process," *IEEE Trans. Wireless Commun.*, vol. 16, no. 11, pp. 7152–7167, Nov. 2017.
[16] N. Deng, W. Zhou, and M. Haenggi, "Heterogeneous cellular network models with dependence," *IEEE J. Sel. Areas Commun.*, vol. 33, no. 10, pp. 2167–2181, Oct. 2015.
[17] M. Sattari and A. Abbasfar, "A novel PHP-based coverage analysis in millimeter wave heterogeneous cellular networks," in *Proc. Iran Workshop Commun. Inf. Theory (IWCIT)*, Tehran, Iran, Apr. 2019, pp. 1–6.
[18] M. A. Kishk and H. S. Dhillon, "Coexistence of RF-powered IoT and a primary wireless network with secrecy guard zones," *IEEE Trans. Wireless Commun.*, vol. 17, no. 3, pp. 1460–1473, Mar. 2018.
[19] M. A. Kishk and H. S. Dhillon, "Modeling and analysis of ambient RF energy harvesting in networks with secrecy guard zones," in *Proc. IEEE Wireless Commun. Netw. Conf. (WCNC)*, San Francisco, CA, USA, Mar. 2017, pp. 1–6.
[20] H. Chen, L. Liu, H. S. Dhillon, and Y. Yi, "QoS-aware D2D cellular networks with spatial spectrum sensing: A stochastic geometry view," *IEEE Trans. Commun.*, vol. 67, no. 5, pp. 3651–3664, May 2019.
[21] M. Afshang and H. S. Dhillon, "Spatial modeling of device-to-device networks: Poisson cluster process meets Poisson hole process," in *Proc. 49th Asilomar Conf. Signals, Syst. Comput.*, Pacific Grove, CA, USA, Nov. 2015, pp. 317–321.
[22] A. H. Sakr and E. Hossain, "Cognitive and energy harvesting-based D2D communication in cellular networks: Stochastic geometry modeling and analysis," *IEEE Trans. Commun.*, vol. 63, no. 5, pp. 1867–1880, May 2015.
[23] A. Al-Hourani, S. Kandeepan, and A. Jamalipour, "Stochastic geometry study on device-to-device communication as a disaster relief solution," *IEEE Trans. Veh. Technol.*, vol. 65, no. 5, pp. 3005–3017, May 2016.
[24] M. Rihan, M. M. Selim, C. Xu, and L. Huang, "D2D communication underlaying UAV on multiple bands in disaster area: Stochastic geometry analysis," *IEEE Access*, vol. 7, pp. 156646–156658, 2019.
[25] A. Jeffrey and D. Zwillinger, *Table of Integrals, Series, and Products*, 7th ed. San Diego, CA, USA: Academic, 2007.
[26] L. Shi, L. Zhao, G. Zheng, Z. Han, and Y. Ye, "Incentive design for cache-enabled D2D underlaid cellular networks using stackelberg game," *IEEE Trans. Veh. Technol.*, vol. 68, no. 1, pp. 765–779, Jan. 2019.
[27] R. Atat, H. Chen, L. Liu, J. Ashdown, M. Medley, and J. Matyjas, "Fundamentals of spatial RF energy harvesting for D2D cellular networks," in *Proc. IEEE Global Commun. Conf. (GLOBECOM)*, Dec. 2016, pp. 1–6.

WENYAN SHI received the B.S. degree from the University of Science and Technology Beijing (USTB), Beijing, China, in 2018. She is currently pursuing the M.S. degree with the School of Information and Communication, Beijing University of Posts and Telecommunications (BUPT), Beijing. Her research interests include cooperative communications and resource allocation for wireless networks.

ZHI ZHANG (Member, IEEE) received the B.S. and Ph.D. degrees from the Beijing University of Posts and Telecommunications (BUPT), Beijing, China, in 1999 and 2004, respectively. He is currently a Professor and a Ph.D. Supervisor with the School of Information and Communication Engineering, BUPT. His research interests include key technology of mobile communications, digital signal processing, and communication system design. He serves as a member for the State Key Laboratory of Networking and Switching Technology, China.

YUZHEN HUANG (Member, IEEE) received the B.S. degree in communications engineering and the Ph.D. degree in communications and information systems from the College of Communications Engineering, PLA University of Science and Technology, in 2008 and 2013, respectively. He is currently an Associate Professor with the Artificial Intelligence Research Center, National Innovation Institute of Defense Technology. He is also a Postdoctoral Research Associate with the School of Information and Communication, Beijing University of Posts and Telecommunications, Beijing. His research interests include channel coding, MIMO communications systems, cooperative communications, physical layer security, and cognitive radio systems. He has published nearly 90 research papers in international journals and conferences. He and his coauthors were awarded the Best Paper Award at the WCSP 2013. He received the IEEE COMMUNICATIONS LETTERS Exemplary Reviewer Certificate in 2014. He serves as an Associate Editor for the *KSII Transactions on Internet and Information Systems*.

WENJUN XU (Senior Member, IEEE) received the B.S. and the Ph.D. degrees from the Beijing University of Posts and Telecommunications (BUPT), Beijing, China, in 2003 and 2008, respectively. He is currently a Professor and a Ph.D. Supervisor with the School of Information and Communication Engineering, BUPT. He serves as the Center Director for the Key Laboratory of Universal Wireless Communications, Ministry of Education, China. He is an Editor of *China Communications*. His research interests include AI-driven networks, UAV communications and networks, green communications and networking, and cognitive radio networks.